Available online at www.worldscientificnews.com

World Scientific News

An International Scientific Journal

WSN 97 (2018) 80-98 EISSN 2392-2192

Synthesis of 2-(5-bromo-2-(2,2,2-trifluoroethoxy) phenyl)-5-aryl-1,3,4-oxadiazoles and their FT-IR, NMR, Mulliken, MEP, HOMO-LUMO and NLO

C. Rajalakshmi and **N. Santhi***

Department of Chemistry, Government Arts College, Chidambaram – 608201, Tamil Nadu, India

*E-mail address: nsaanthi@gmail.com

ABSTRACT

A series of novel 2-(5-bromo-2-(2,2,2-trifluoroethoxy)phenyl)-5-aryl-1,3,4-oxadiazole (**3a-e**) were synthesized and confirmed by spectral analyses. The optimized structure with their bonding aspects and vibrational frequencies of the same have been examined utilizing DFT-B3LYP technique with a basis set 6-31G(d,p). In the optimized structures of compounds **3a-e**, the bond lengths and bond angles are in accord with their corresponding reported analogous. The vibrational frequencies resulted from experimental as well as theoretical are in well accord with each other. Furthermore, Mulliken charge and MEP analyses of the compound have been calculated in order to get insight into the compound. The quantum chemical descriptors such as HOMO and LUMO energies were used to analyze the charge transfer within the molecule. In addition, the results of polarizabilities, first order hyperpolarizabilities and dipole moment of title compounds imply that these could be utilized for the preparation of NLO crystals.

***Keywords*:** 1,3,4-oxadiazoles, FT-IR, hyperpolarizability, HOMO –LUMO

1. INTRODUCTION

Oxadiazoles are among the most prevalent heterocycles in biologically active compounds. Of course, numerous oxadiazoles derivatives possess potent biological activities including ntiinflammatory [1-4], hypoglycemic [5,6], antianxiety, antidepressant [7], and

(Received 24 March 2018; Accepted 08 April 2018; Date of Publication 09 April 2018)

antimitotic [8] activities. In addition to these, a number of researchers have reported antimicrobial activities [9-13]. A minority example of oxadiazole-based compounds have been recently used as electron transport materials [14-19] in organic light emitting diodes (OLEDs) Nowadays, the recognition and discovery of environmentally and biologically important analytes has become an essential research topic in chemistry and biology. Among different analytical methods, optical measurements in conjunction with suitable biological activity are preferable approaches for detection, because they are convenient, low cost, non-destructive, and highly sensitive and selective to analytes.

The importance of the oxadiazoles functionality in biologically active compounds has fused research into the development of new protocols for the synthesis and study of their molecular structural properties, electronic and polarizability data of oxadiazoles, in gas phase, due to its pharmaceutical importance. A series of derivatives of oxadiazoles were synthesized and tested, revealing precise requirements for activity in tight and relatively level molecular structural properties, electronic and polarizability.

The unaltered 5-bromo-2-(2,2,2-trifluoroethoxy)phenyl core was shown to be optimal for activity while certain modifications to the phenyl ring were tolerated. The ground state properties of the modified molecules are calculated using DFT/B3LYP level of theory using 6-31G(d,p) basis set. We therefore wished to investigate and examine their molecular structure, FT-IR, dipole moment, polarizability, first order hyperpolarizability, HOMO–LUMO, Mulliken population analysis along with the molecular electrostatic potential surface.

2. EXPERIMENTAL

2. 1. General Procedure for the Synthesis of 2-(5-bromo-2-(2,2,2-trifluoroethoxy) phenyl)-5-aryl-1,3,4-oxadiazole (3a-e)

In a round bottom flask, aryl hydrazide **1(a-e)** was dissolved in phosphorous oxychloride (5 mL) and to it equimolar amount of 5-bromo-2-(2,2,2-trifluoroethoxy)benzoic acid **2** was added. This mixture was refluxed at mild condition. After completion of the reaction, the mixture was cooled to room temperature and poured onto crushed ice. On neutralization of the contents with sodium bicarbonate solution (20%), a solid mass separated out. This was filtered and washed with water. It was crystallized by using methanol to give **3a-e**. The synthetic route is given **Scheme 1.**

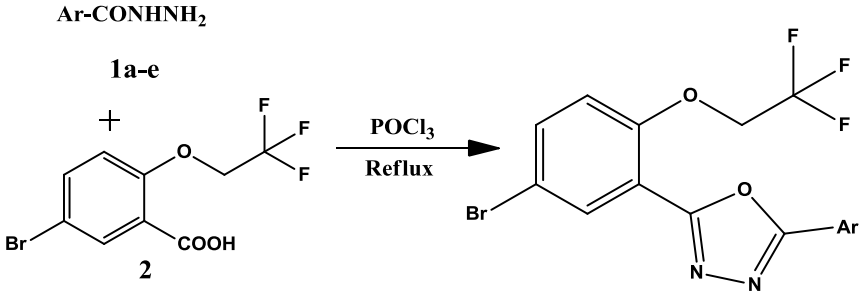

Entry	Ar
3a	C_6H_5
3b	C_6H_4Cl
3c	$C_6H_4NO_2$
3d	C_6H_4Br
3e	C_5H_4N

Scheme 1.

2. 2. Spectral measurements

The FT-IR spectrum of the synthesized compounds was measured in the range 4000-500 cm^{-1} on a AVATAR-330 FT-IR spectrometer (Thermo Nicolet) using KBr (pellet form). ^{1}H NMR spectrum was recorded at 400 MHz on a BRUKER and for ^{13}C NMR spectrum was recorded at 100 MHz on a BRUKER model using $CDCl_3$ as solvent. Tetramethylsilane (TMS) was used as internal reference for all NMR spectra, with chemical shifts reported in δ units (parts per million) relative to the standard.

2-(5-bromo-2-(2,2,2-trifluoroethoxy)phenyl)-5-phenyl-1,3,4-oxadiazole (3a).
Yield 76%, white powder, mp (°C): 240-242; IR (cm^{-1}): 3072 (ν_{ArC-H}), 2922 ($\nu_{Ali.C-H}$), 1587 ($\nu_{C=N}$), 1063 ($\nu_{C–O–C}$), 1271 (ν_{C-F}), 1275-1245 (β_{C-H}), 1063-818; ^{1}H NMR ($CDCl_3$, 400 MHz, ppm): 4.77 (s, 2H), 6.94-8.16 (m, 2H, Ar-H); ^{13}C NMR ($CDCl_3$); 154.5 (C-5), 165.3 (C-9), 161.7 (C-12), 67.7 (C-15).

2-(5-bromo-2-(2,2,2-trifluoroethoxy)phenyl)-5-(4-chlorophenyl)-1,3,4-oxadiazole (3b).
Yield 75%, white powder, mp (°C): 240–242; IR (cm^{-1}): 3076 (ν_{ArC-H}), 2946 ($\nu_{Ali.C-H}$), 1575 ($\nu_{C=N}$), 1059 ($\nu_{C–O–C}$), 1277 (ν_{C-F}), 12491179 (β_{C-H}), 1059-796; ^{1}H NMR ($CDCl_3$, 400 MHz, ppm): 4.53 (s, 2H), 6.93-8.34 (m, 2H, Ar-H); ^{13}C NMR ($CDCl_3$); 154.0 (C-5), 164.5 (C-9), 163.9 (C-12), 67.5 (C-15).

2-(5-bromo-2-(2,2,2-trifluoroethoxy)phenyl)-5-(4-nitrophenyl)-1,3,4-oxadiazole (3c).
Yield 75%, white powder, mp (°C): 240–242; IR (cm^{-1}): 3099 (ν_{ArC-H}), 2954 ($\nu_{Ali.C-H}$), 1584 ($\nu_{C=N}$), 1066 ($\nu_{C–O–C}$), 1291 (ν_{C-F}), 1291,1267 (β_{C-H}), 1107-739; ^{1}H NMR ($CDCl_3$, 400 MHz, ppm): 4.54 (s, 2H), 6.94-8.43 (m, 2H, Ar-H); ^{13}C NMR ($CDCl_3$); 154.5 (C-5), 163.6 (C-9), 161.7 (C-12), 67.5 (C-15).

2-(5-bromo-2-(2,2,2-trifluoroethoxy)phenyl)-5-(3-bromophenyl)-1,3,4-oxadiazole (3d).
Yield 78%, white powder, mp (°C): 240–242; IR (cm^{-1}): 3071 (ν_{ArC-H}), 2922 (ν_{AliC-H}), 1604 ($\nu_{C=N}$), 1063 ($\nu_{C–O–C}$), 1292 (ν_{C-F}), 1267,1246 (β_{C-H}), 1071-815; ^{1}H NMR ($CDCl_3$, 400 MHz, ppm): 4.51 (s, 2H), 6.93-8.33 (m, 2H, Ar-H); ^{13}C NMR ($CDCl_3$); 154.5 (C-5), 164.0 (C-9), 162.0 (C-12), 67.1 (C-15).

2-(5-bromo-2-(2,2,2-trifluoroethoxy)phenyl)-5-(pyridin-4-yl)-1,3,4-oxadiazole (3e).
Yield 68%, white powder, mp (°C): 240–242; IR (cm^{-1}): 3098 (ν_{ArC-H}), 2922 ($\nu_{Ali.C-H}$), 1595 ($\nu_{C=N}$), 1059 ($\nu_{C–O–C}$), 1295 (ν_{C-F}), 1269,1247 (β_{C-H}), 1058-818; ^{1}H NMR ($CDCl_3$, 400 MHz, ppm): 4.50 (s, 2H), 6.87-8.76 (m, 2H, Ar-H); ^{13}C NMR ($CDCl_3$); 151.4 (C-5), 164.8 (C-9), 159.1 (C-12), 57.6 (C-15).

2. 3. Computational studies

GAUSSIAN 03W [20] software package was used for DFT calculations. Structure optimizations of **3a-e** were performed at the Density Functional Theory (DFT) level employing B3LYP/6-31G(d,p) functional theory. In addition, virational analysis of title compounds were also studied by same mentioned level theory. In order examine the reactive sites of the synthesized compounds; the Mulliken and molecular electrostatic potential were evaluated. Moreover, in order to show nonlinear optical (NLO) activity of studied molecules,

the dipole moment, linear polarizability and first order hyperpolarizability were obtained from molecular polarizabilities based on same level theoretical calculations. Also, the HOMO-LUMO on optimized structures is accomplished at B3LYP/6-31G(d,p) level computation. Numbering Pattern compounds of **3a-e** is shown **Fig. 1.**

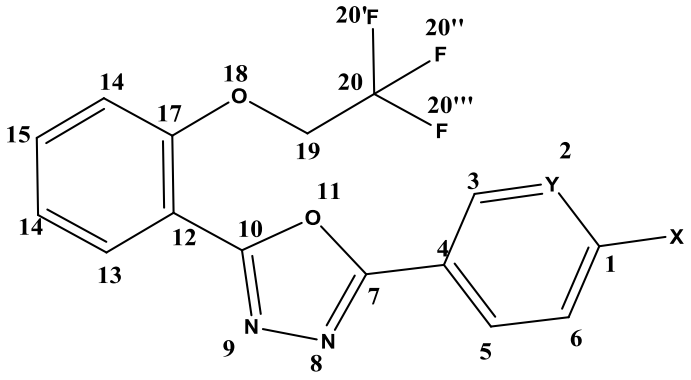

Entry	X	Y
3a	H	CH
3b	Cl	CH
3c	NO_2	CH
3d	H	CBr
3e	H	N

Fig. 1. Numbering Pattern of **3a-e**.

3. RESULTS AND DISCUSSION

3. 1. Geometry optimization

The optimized bond lengths, bond angles and dihedral angles of compound **3a-e** obtained by B3LYP/6-31G(d,p) level are compiled in **Table 1**. The optimized structure of title compounds are displayed in **Fig. 2**. The title compounds (**3a-e**) consist of three rings, namely 5-bromo-2-(2,2,2-trifluoroethoxy)phenyl, oxadiazole and substituted phenyl.

The theoretical values obtained by DFT method were compared with the available experimental one, most of the optimized bond lengths were in excellent agreement with the structural parameters.

Table 1. Optimized parameter of oxadiazoles **3a-e**

Bond length (Å)	3a	3b	3c	3d	3e
C1-Y2	1.395	1.395	1.401	1.395	1.41
C1-X1	1.1	1.76	1.47	1.07	1.07
Y2-C3	1.395	1.395	1.401	1.395	1.398
C3-C4	1.395	1.395	1.401	1.395	1.395
C4-C5	1.395	1.395	1.401	1.395	1.388
C5-C6	1.395	1.395	1.401	1.395	1.401

C4-C7	1.498	1.54	1.49	1.54	1481
C7-N8	1.372	1.372	1.383	1.392	1.325
N8-N9	1.518	1.522	1.398	1.522	1.519
N9-C10	1.372	1.322	1.393	1.362	1.382
C10-O11	1.522	1.522	1.432	1.522	1.522
O11-C7	1.522	1.522	1.432	1.522	1.522
C10-C12	1.54	1.54	1.54	1.54	1.54
C12-C13	1.395	1.395	1.401	1.395	1.395
C13-C14	1.395	1.395	1.401	1.395	1.395
C14-Br14	1.91	1.91	1.91	1.91	1.91
C14-C15	1.395	1.395	1.395	1.395	1.395
C15-C16	1.395	1.395	1.395	1.395	1.395
C16-C17	1.395	1.395	1.395	1.395	1.395
C17-C12	1.395	1.395	1.395	1.395	1.395
C17-O18	1.43	1.43	1.43	1.42	1.43
O18-C19	1.432	1.43	1.43	1.428	1.43
C19-C20	1.54	1.54	1.54	1.539	1.54
C20-F20'	1.35	1.35	1.35	1.35	1.35
C20-F20"	1.35	1.35	1.35	1.35	1.35
C20-F20"'	1.35	1.35	1.35	1.35	1.35
Bond angle (°)					
C3-C4-C7	120	120	120	120	120
C5-C4-C7	120	120	120	120	120
N9-C10-C12	110.5	110.5	123.9	110.5	110.5
O11-C10-C12	110.5	110.5	123.9	110.5	110.5
C13-C12-C10	119.8	120	118.9	120	120.4
C13-C14-C15	120	120	120	120	120

C13-C14-Br14	120	120	120.3	120	119.5
C15-C14-Br14	119.8	120	120.4	119.3	120
C17-C12-C10	120	120	120	120	120
O18-C17-C16	120	120	119.8	120	118.9
O18-C17-C12	118.5	120	121.4	120	118.6
Dihedral (°)					
C3-C4-C7-O11	60.9	61	60.7	60.9	60.7
C5-C4-C7-O11	-119.2	-119.2	179.8	-119.2	-180
C3-C4-C7-N8	180	180	179.8	180	180
C5-C4-C7-N8	0.1	0.5	0.2	4.3	4.8
C10-C12-C17-O11	0.2	8.6	1.5	6.8	1.8
C17-C12-C10-O11	106	106	106	106	106
C17-C12-C10-N9	-134.5	-134.5	-134.5	-134.5	-134.5
O18-C17-C16-C15	180	180	180	180	180
O18-C17-C12-C10	1.2	4.5	8.4	1.5	8.5

X – H, Cl and N for compound s **3a-e**.
Y = H, C-Br, N for compound s **3a-e**

The aromatic bond distances in the title compounds are observed in the interval 1.388-1.40 Å, which is well matched with XRD value [21]. The experimental N-N and C-O bond lengths being long, they might be linked to the intermolecular hydrogen bonds. The C-H and C-F bond length differences might be due to low scattering factors of hydrogen atoms in X-Ray diffraction [22,23].

The selected bond distances are C7-N8 and C10-N9 (~1.37 Å) having double bond character, which is well matched with 1.35 Å (XRD) value [21]. A comparison between the experimental and the calculated values reveal that there are marginal differences between the two. The differences may be due to the fact that the theoretical values were for a gaseous molecule whereas experimental values were for the molecule in the solid state associated with intermolecular interactions.

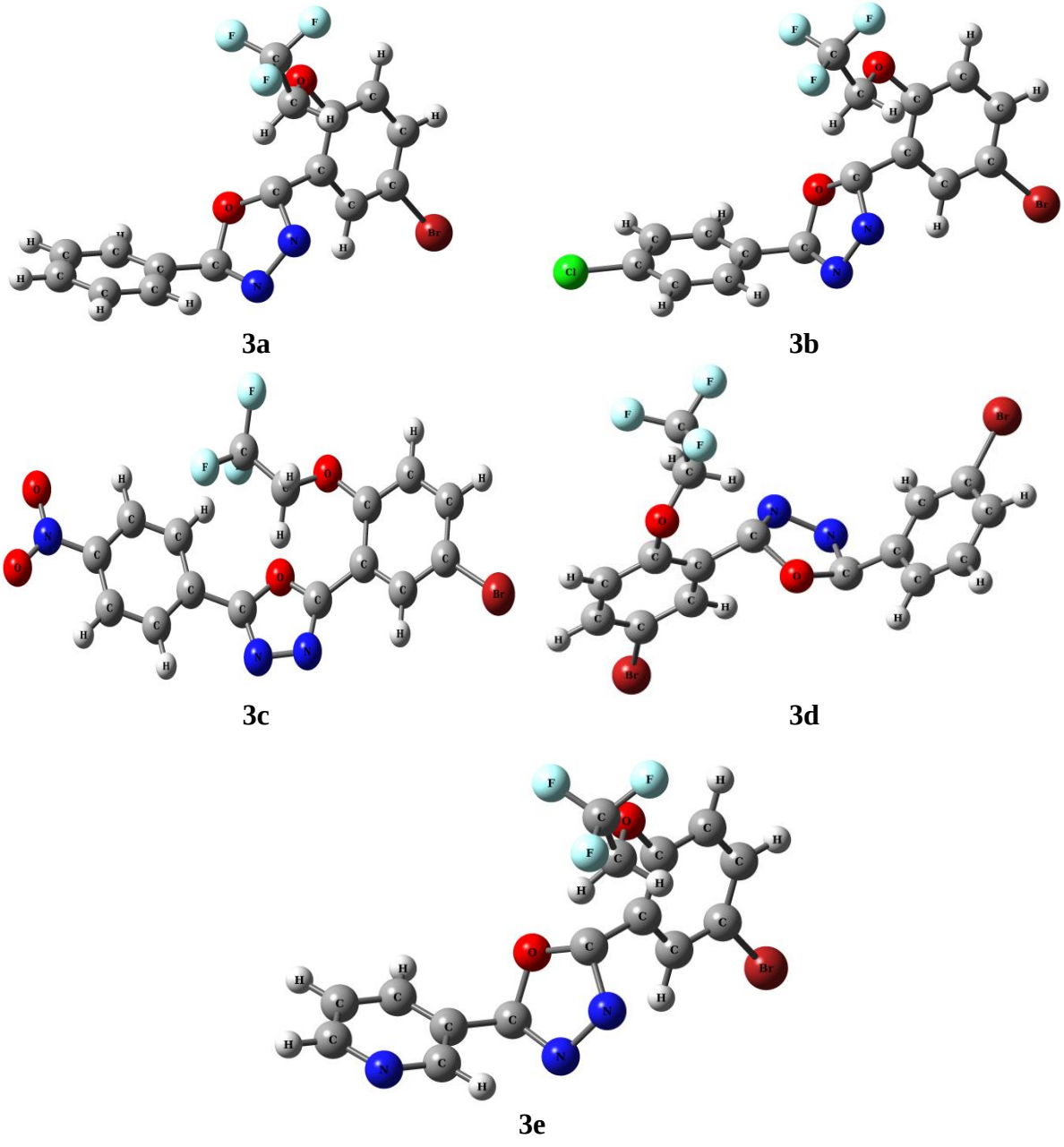

Fig. 2. Optimized structure of oxadiazoles **3a-e**

3. 2. Infrared spectral analysis

The experimental and calculated FT-IR spectra of the molecule **3a** are shown in Figs. 3a and b. The theoretical frequencies computed at B3LYP method with 6-31G(d,p) basis set along with their relative intensities, plausible assignments are summarized in **Table 2**. Generally the calculated harmonic vibrational wavenumbers are higher than the experimental ones. This is because of the anharmonicity of the incomplete treatment of electron correlation and of the use of finite one-particle basis set. Hence the theoretical harmonic vibrational wavenumbers are scaled

by 0.9608 [24]. After applying a uniform scaling factor, the theoretical calculation reproduces the experimental data well. The experimental FT-IR spectrum of compounds **3a-e** show aromatic C-H stretching vibrations in the interval 3072-3099 cm^{-1}, whereas the computed scaled vibrations assigned in the range 3101 to 3076 cm^{-1}. The methyl and methylene groups stretching are expected at 2980-2870 cm^{-1} [25]. The C-H stretching of these groups appeared around 2954 cm^{-1} as very strong bands in FT-IR and its corresponding DFT values ranges from 3001 to 2937 cm^{-1}. In the present case a strong band around 1587 cm^{-1} is ascribed to C=N stretching vibration, which is consistent with the calculated frequency at 1598 cm^{-1}. The C-O stretching vibration occurs ~ 1066 cm^{-1} in FT-IR.

Table 2. Experimental and calculated IR frequencies of compounds **3a-e**

Assignments	**3a**			**3b**			**3c**		
	FT-IR	DFT		FT-IR	DFT		FT-IR	DFT	
		Scaled	Intensity		Scaled	Intensity		Scaled	Intensity
$\nu_{ar\cdot C-H}$	3072	3076	43.19	3076	3098	52.43	3099	3101	21.43
$\nu_{ali\cdot C-H}$	2922	2937	23.47	2946	3001	32.07	2954	2981	5.40
$\nu_{C=N}$	1587	1598	101.53	1575	1587	98.63	1584	1585	98.03
$\nu_{C=C}$	1545	1568	6.34	1543	1567	4.34	1553	1561	14.45
	1537	1553	138.93	-	-	-	1476	1481	121.43
	1477	1495	30.84	1447	1472	45.80	1457	1457	21.80
ν_{C-F}	1271	1287	74.55	1277	1281	68.50	1291	1301	70.52
ν_{C-O}	1063	1078	6.23	1059	1065	0.23	1066	1067	12.23
β_{C-H}	1275	1284	16.32	1249	1251	43.21	1291	1291	16.32
	1245	1275	2.17	1179	1184	11.07	1267	1253	1.17
Γ_{C-H}	1063	1094	8.26	1059	1065	13.26	1107	1131	12.26
	969	1014	5.74	971	996	2.70	970	971	0.74
	898	916	8.67	885	914	15.87	857	857	4.07
	864	875	18.35	816	824	19.37	818	828	17.34
	818	824	8.83	796	810	10.42	739	741	6.41
ν_{C-Cl}	-	-	-	752	761	8.45	-	-	-

Table 2(continue). Experimental and calculated IR frequencies of compounds **3a-e**

Assignments	3d			3e		
	FT-IR	DFT		FT-IR	DFT	
		Scaled	Intensity		Scaled	Intensity
$\nu_{ar\cdot C-H}$	3071	3083	22.12	3098	3101	52.21
$\nu_{ali\cdot C-H}$	2923	2941	20.47	2922	2934	30.43
$\nu_{C=N}$	1604	1652	141.53	1595	1595	118.62
$\nu_{C=C}$	1545	1556	0.34	1467	1456	14.34
	1478	1481	98.96	-	-	-
	1458	1481	40.80	-	-	-
ν_{C-F}	1292	1293	74.55	1295	1299	11.07
ν_{C-O}	1063	1064	3.23	1059	1061	13.26
β_{C-H}	1267	1267	18.32	1269	1268	2.70
	1246	1242	8.18	1247	1256	15.87
Γ_{C-H}	1071	1075	2.26	1058	1061	19.37
	1011	1011	14.74	969	971	2.70
	884	884	21.60	864	871	15.87
	862	871	8.35	818	824	18.37
	815	832	13.84	818	821	16.40
ν_{C-Cl}	-	-	-	-	-	-

The computed value well correlates well with measured FT-IR value [26,27]. The title molecules show experimental C=C stretching vibrations in the region 1553-1447 cm^{-1}. Theoretically computed scaled C=C stretching vibrations by DFT method appeared at between 1568-1457 cm^{-1}. The NO_2 stretching vibrations in FTIR spectrum of 3c is mixed with C=C stretching vibrations. An intense band around 1271 cm^{-1} in the IR spectrum was a characteristic out of plane C-F vibration of compounds **3a-e** [27].

Meanwhile the frequencies for (βring-H) aromatic ring were recorded around ~1245-1175 cm^{-1} for the title compounds. These values are in accordance with those reported in the literature [26,27].

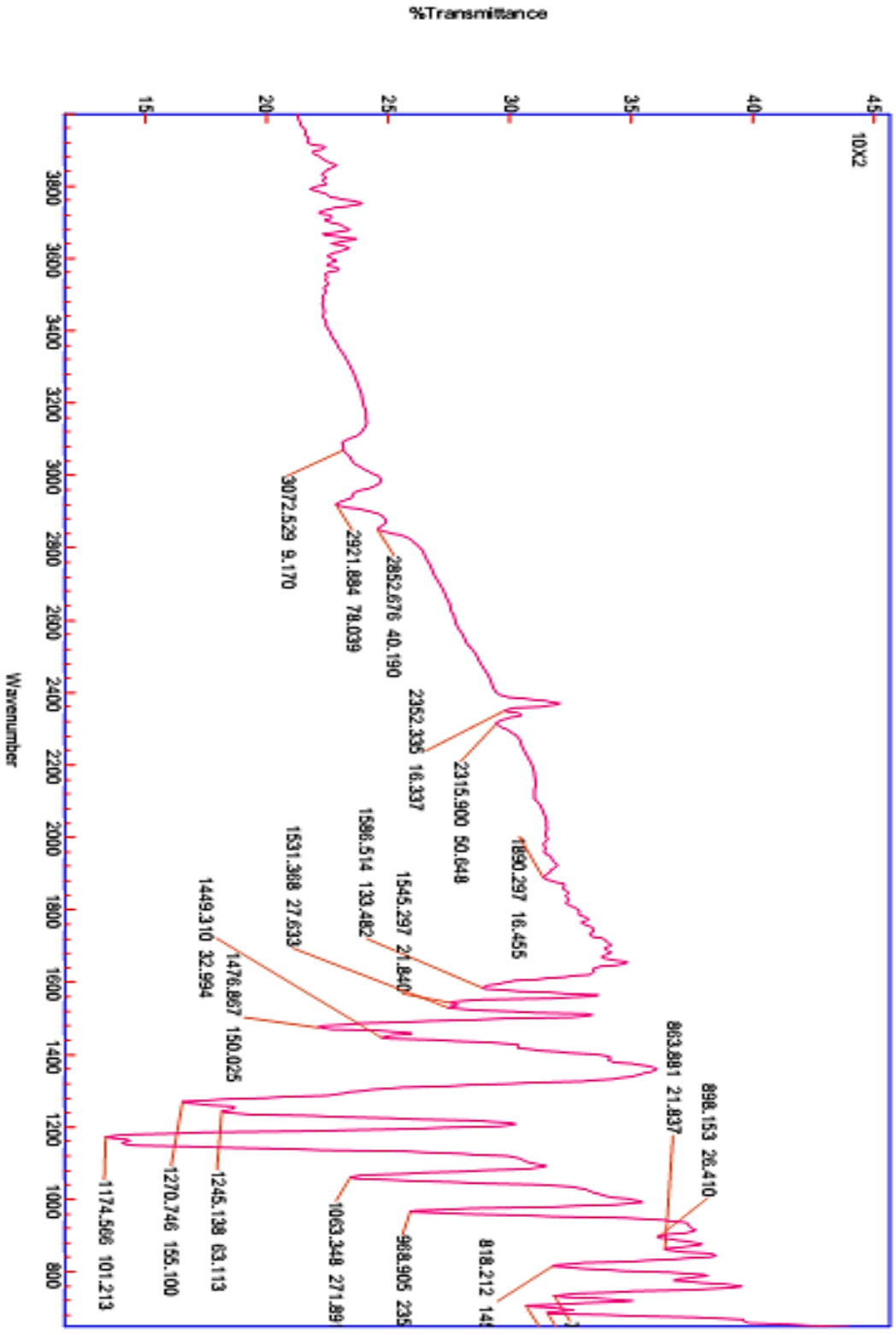
%Transmittance
10X2
Wavenumber
3072.529 9.170
2921.884 78.039
2852.676 40.190
2352.335 16.337
2315.900 50.648
1690.297 16.455
1586.514 133.482
1545.297 21.840
1531.368 27.633
1449.310 32.994
1476.867 150.025
1245.138 63.113
1270.746 155.100
1174.566 101.213
1063.348 271.89
968.905 235
898.153 26.410
863.881 21.837
818.212 14

(a)

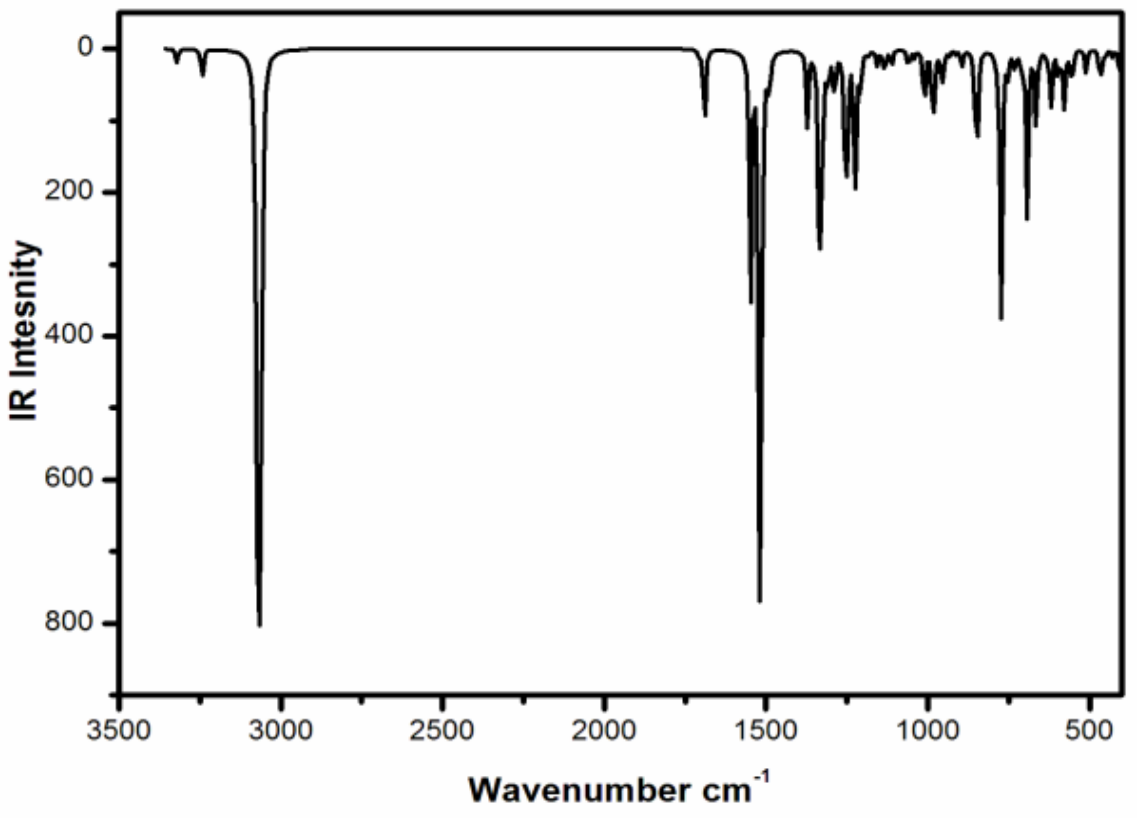

(b)

Figs. 3. (a) FT-IR and **(b)** computed IR spectra of compound **3a**

3. 3. Analysis of Mulliken population

The atomic charges title molecules compounds acquired by Mulliken charge analysis with DFT method have been given in **Table 3**. Atomic charges have been utilized to illustrate the process of equalization of electro negativity and transfer of charge in chemical reactions [28,29]. The result shows that most of the carbon atoms in molecules **3a-e** accommodate negative charges lead to a reorganization of electron density. The carbon atoms such as C7, C10, C14, C17, and C20, which are directly connected to the electronegative atoms, hold elevated positive charge and as a result of the same, they become greater acidic. These data clearly show that oxadiazoles are the most reactive towards substitution reactions.

Table 3. Mulliken atomic charges of **3a-e**.

Atoms	**3a**	**3b**	**3c**	**3d**	**3e**
C1	-0.106	-0.257	0.357	-0.074	0.043
X1	0.143	0.137	0.05	0.157	0.167

Y2	-0.14	-0.112	-0.145	-0.33	-0.405
C3	-0.102	-0.09	-0.16	-0.073	0.036
C4	0.025	0.018	0.145	0.036	0.025
C5	-0.109	-0.1	-0.157	-0.106	-0.079
C6	-0.14	-0.111	-0.13	-0.124	-0.133
C7	0.248	0.255	0.249	0.251	0.251
N8	-0.211	-0.212	-0.245	-0.212	-0.211
N9	-0.188	-0.187	-0.255	-0.187	-0.181
C10	0.181	0.174	0.271	0.174	0.179
O11	-0.41	-0.399	-0.415	-0.399	-0.408
C12	0.088	0.089	0.188	0.089	0.089
C13	-0.082	-0.083	-0.105	-0.083	-0.083
C14	0.319	0.318	0.329	0.319	0.319
Br14	0.18	0.182	0.19	0.18	0.184
C15	-0.093	-0.092	-0.07	-0.093	-0.094
C16	-0.117	-0.116	-0.123	-0.117	-0.117
C17	0.252	0.258	0.236	0.252	0.252
O18	-0.526	-0.525	-0.49	-0.526	-0.526
C19	-0.116	-0.112	-0.113	-0.114	-0.115
C20	0.763	0.765	0.765	0.765	0.766
F20'	-0.262	-0.263	-0.255	-0.262	-0.262
F20"	-0.258	-0.259	-0.275	-0.259	-0.265
F20"'	-0.266	-0.266	-0.258	-0.265	-0.259

X – H, Cl and N for compounds **3a-e**.
Y = H, C-Br, N for compounds **3a-e**

3. 4. Molecular electrostatic potential (MEP) analysis

MEP is an important tool used to predict the reactivity of a wide variety of chemical systems in both electrophilic and nucleophilic reactions [30-32]. It provides a visual method

to understand the relative polarity of the molecule. Fig. 4 shows the MEP surface plot for the title molecules. The deepest blue density which represents the electron deficient regions and deepest red density represents the electron rich regions in the plot. The green area represents the zero electrostatic potential regions.

It is seen from Fig. 4 that the region around nitrogen, oxygen and fluorine atoms linked with carbon through double bond represents the most negative potential region (red) and the region around the hydrogen represents the maximum positive charge (blue) in molecule. These negative and positive sites provide information concerning the region from where the compound can have intermolecular interactions and metallic bondings [33].

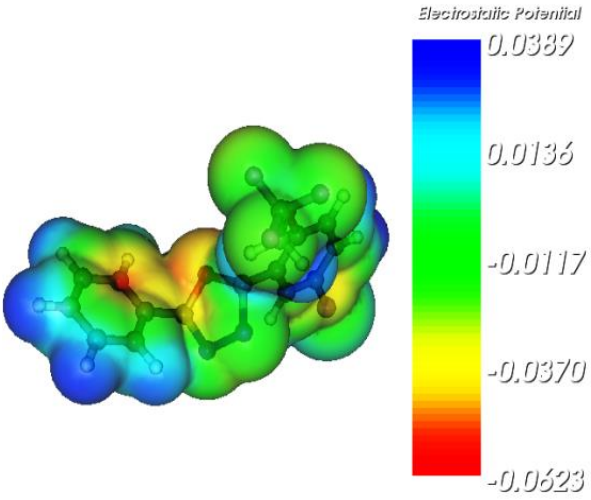

3a

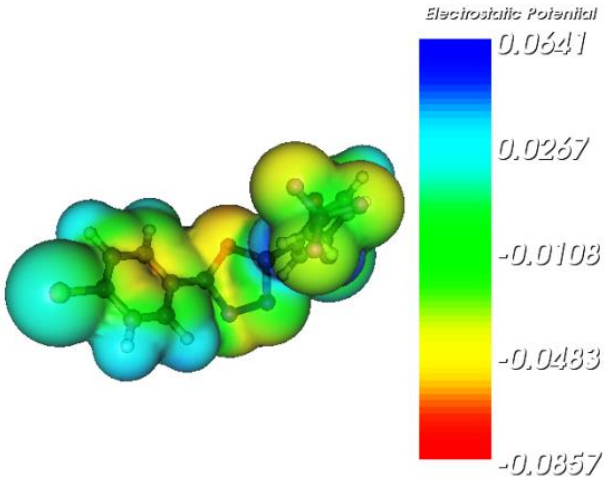

3b

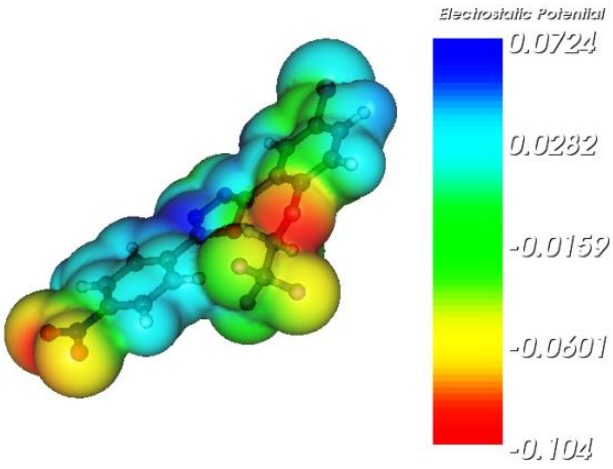

3c

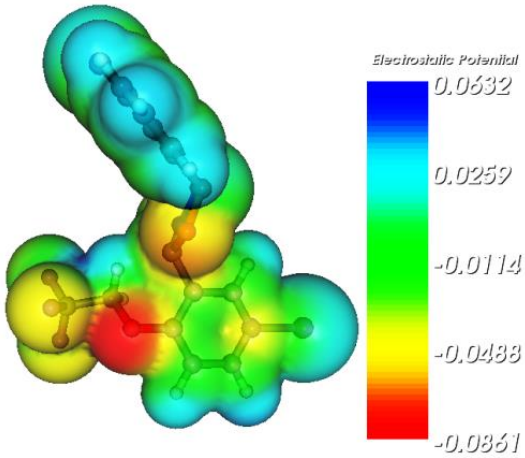

3d

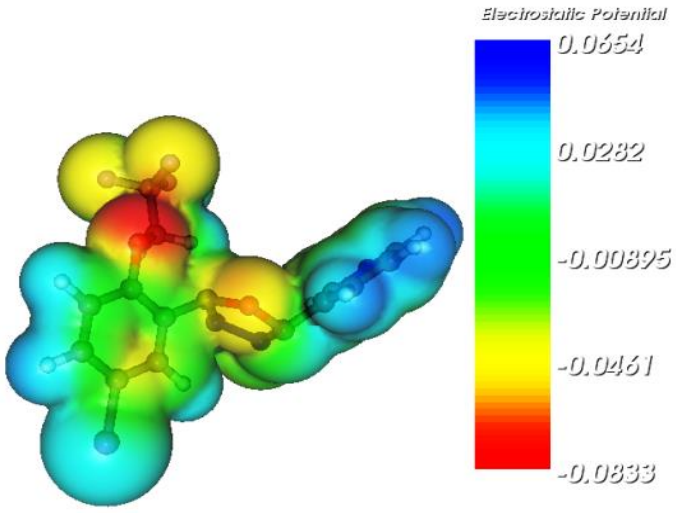

3e

Fig. 4. MEP diagram of **3a-e**

3. 5. Frontier molecular orbital analysis

The highest occupied molecular orbitals (HOMOs) and the lowest unoccupied molecular orbitals (LUMOs) are labelled as frontier molecular orbitals (FMOs) as they appear at the outermost boundaries of the electrons in a molecule. Basically the HOMO describes the electron donating ability and the LUMO describes the electron accepting ability of a molecule. The energy gap between the HOMO and LUMO determines the chemical stability of a molecule [34-36] and also explains the charge transfer interactions within the molecule. HOMO-LUMO orbitals of the compounds **3a-e** are computed in the gaseous phase using B3LYP method with 6-31G (d,p) basis set. The 3D surface plots of HOMO and LUMO are shown in **Fig. 5**. The energy gap is an important parameter in determining molecular electrical transport properties [37] which helps in predicting the most reactive position in conjugated system and also describes several types of reaction in conjugated system [38]. The conjugated molecules show a small HOMO-LUMO energy gap, which indicates that a significant degree of intramolecular charge transfer from electron donor groups to electron acceptor groups through p system which is very good for nonlinear optical applications [39,40]. Furthermore, the difference on the values of ΔE of compounds **3a-e** was observed, which has different substituent at 1-site of the phenyl core. The HOMO-LUMO gaps lie over a range of 3.00 to 3.16 eV. The increasing order of HOMO-LUMO energy gap is as follows **3e** < **3d** < **3b** < **3a** < **3c**. Results from HOMO and LUMO energy values, the quantum chemical reactivity descriptors such as hardness, chemical potential, electronegativity and electrophilicity index as well as local reactivity have been defined [41] Pauling introduced the idea of electronegativity as the power of an atom in a molecule to attract electrons to it. Hardness (η), chemical potential (η) and electronegativity (χ) are defined using Koopman's theorem as $\eta = (I - A)/2$, $\mu = -(I + A)/2$ and $\chi = (I + A)/2$, where $I = -E_{HOMO}$ and $A = -E_{LUMO}$ are the ionization potential and electron affinity of the molecule.

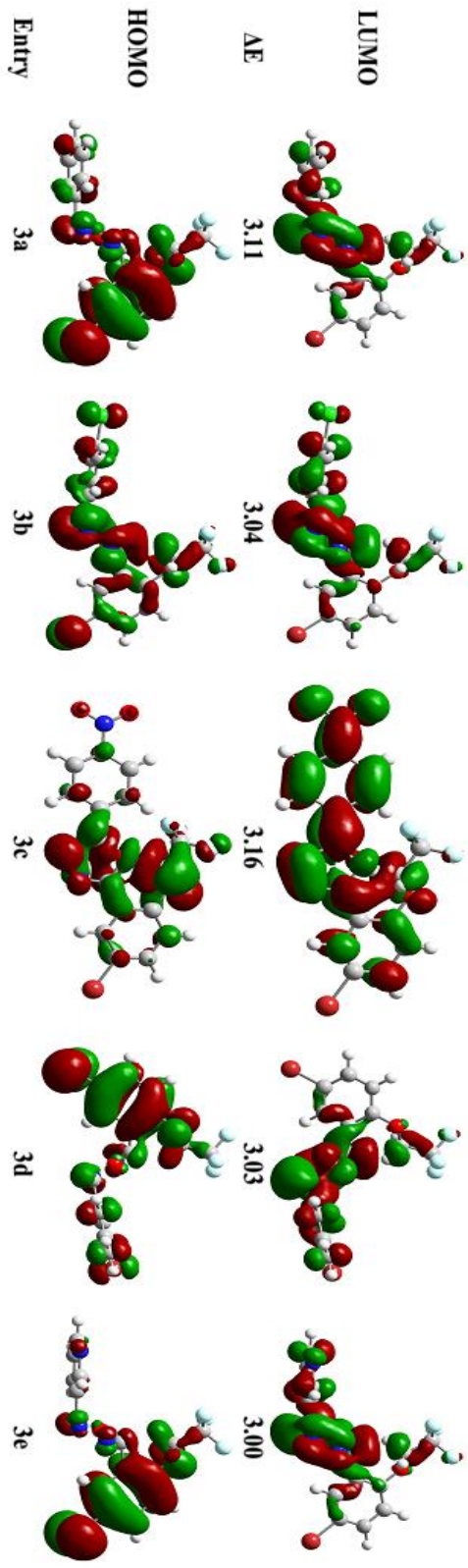

Fig. 5. Molecular orbitals and energies for the HOMO and LUMO in gas phase.

Table 4. Calculated energy values (eV) of **3a-e** in gas phase.

DFT-B3LYP/6-31G(d,p)	**3a**	**3b**	**3c**	**3d**	**3e**
E_{HOMO}	-6.87	-6.96	-6.62	-6.96	-6.96
E_{LUOMO}	-3.76	-3.92	-3.47	-3.93	-3.96
ELUMO-HOMO	3.11	3.04	3.16	3.03	3.00
Electronegativity(χ)	-5.32	-5.44	-5.55	-5.45	-5.47
Hardness(η)	1.56	1.52	2.08	1.51	1.51
Electrophilicity index(ψ)	9.09	9.75	7.40	9.80	9.89
Softness(s)	237.87	243.60	178.16	244.74	244.41

Global electronegativity values of investigated molecules are given in **Table 4**. From **Table 4**, the **3c** molecule has the bigger electronegativity. Hence, electronegativity of **3c** molecule carrying nitro group in *para*-position has affected on the entire of molecular structure. Chemical hardness is connected with the stability and reactivity of a chemical system, it measures the resistance to change in the electron distribution or charge transfer. In this sense, chemical hardness corresponds to the gap between the HOMO and LUMO.

The larger the HOMO–LUMO energy gap, the harder and more stable/less reactive the molecule. The higher value of ΔE represents more hardness or less softness of a compound, thus compound **3c** referred as hard molecule when compared to other compounds**.**

3. 6. Non-linear optical characteristics

Table 5. Non-linear optical properties of **3a-e**calculated using B3LYP method using 6-31G(d,p) basis set.

NLO behavior	**3a**	**3b**	**3c**	**3d**	**3e**
Dipole moment (μ) D	2.02	1.71	6.09	2.63	3.43
Mean polarizabilty (α) $\times 10^{-23}$ esu	2.14	2.42	2.69	2.44	2.20
Anisotropy of the Polarisabiltiy (Δα) $\times 10^{-24}$ esu	5.91	2.93	6.86	4.45	5.72
First order polarizabilty (β_0) $\times 10^{-30}$ esu	0.83	2.71	6.54	0.45	1.97

For investigating the relationship between non-linear optical properties (NLO) and molecular structures, the polarizabilities as well as first order hyperpolarizabilities have been calculated. It is recognized that molecules possessing superior dipole moment, molecular polarizability and first hyperpolarizability show greater non-linear optical behaviors [42].

In this sense, in this study the electronic dipole moment, mean polarizabilty, anisotropy of the polarisabiltiy and first order polarizabilty of present compounds were investigated. The design of NLO switches, that is, molecules computed for their first hyperpolarizability by alternate their substitution at 1- site in phenyl core.

The total static dipolemoment (μ), the Mean polarizabilty (α), Anisotropy of the polarisabiltiy (Δα) and the first order hyperpolarizability (β_0) using the x, y, z components are calculated using the following equations.

$$\mu = (\mu_x^2 + \mu_y^2 + \mu_z^2)^{1/2}$$

$$\alpha_{tot} = \frac{1}{3}\alpha_{xx} + \alpha_{yy} + \alpha_{zz}$$

$$\Delta\alpha = \frac{1}{\sqrt{2}}\left[(\alpha_{xx} - \alpha_{yy})^2 + (\alpha_{yy} - \alpha_{zz})^2 + (\alpha_{zz} - \alpha_{xx})^2 + 6(\alpha_{xy}^2 + \alpha_{yz}^2 + \alpha_{xz}^2)\right]^{1/2}$$

$$\beta_0 = [(\beta_{xxx} + \beta_{xyy} + \beta_{xzz})^2 + (\beta_{yyy} + \beta_{yzz} + \beta_{yxx})^2 + (\beta_{zzz} + \beta_{zxx} + \beta_{zyy})^2]^{1/2}$$

The first hyperpolarizability (β_0) of compounds **3a-e** is obtained in the interval 0.45-6.54×10^{-30} esu. Further, the first hyperpolarizability values of the title compounds are compared with urea (0.372×10^{-30} esu). The hyperpolarizability values of designed compounds are higher compared to urea [43]. As seen from **Table 5**, the dipole-moments of title compounds are also greater when compared with urea (1.373 Debye). The aforementioned results imply that the molecular polarizability as well as hyperpolarizability of the synthesized compounds **3a-e** in all coordinates are active and hence they could be utilized for the preparation of non-linear optical crystals which might generate second order harmonic waves.

4. CONCLUSIONS

The optimized structural parameters (bond length, bond angle and dihedral angles) are calculated and analyzed by B3LYP level of theory utilizing 6-31G(d,p) basis set. The optimized results are good agreement with reported crystal data. The FT-IR frequencies obtained experimentally are compared with the theoretically calculated wave numbers and are in harmony with each other. The small ΔE between the HOMO and LUMO of the title compounds enlighten the happening of ultimate transfer of charge within the molecule. The molecular orbitals, molecular electrostatic potential surface and NLO analysis direct to the understanding of various properties of the molecules synthesized. The synthesized molecules could be utilized for the preparation of NLO crystals which might generate second order harmonic waves.

References

[1] F.A. Omar, N.M. Mehfouz, M.A. Rahman, *Eur. J. Med. Chem.* 31 (1996) 819.

[2] E. Palaska, G. Sahin, P. Kelicen, N.T. Durlu, G. Altinok, *IL Farmaco* 57 (2002) 101.

[3] T. Ramalingum, P.B. Sattur, *Eur. J. Med. Chem.* 25 (1990) 541.

[4] K. Raman, K.H. Singh, S.K. Satzman, S.S. Parmar, *J. Pharm. Sci.* 82 (1993) 167.

[5] M.M. Girges, *Arzneim-Forsch* 44 (1994) 490.

[6] M.I. Husain, A. Kumar, R.C. Srivastava, *Curr. Sci.* 55 (1986) 644.

[7] M. Harfenist, D.J. Heuser, C.T. Joyner, J.F. Batchelor, H.L. White, *J. Med. Chem.* 39 (1996) 1857.

[8] K.M.L. Rai, N. Linganna, *IL Farmaco* 55 (2000) 389.

[9] S. Giri, H. Singh, L.D.S. Yadav, *Agr. Biol. Chem.* 40 (1976) 17.

[10] Mir, M.T. Siddiqui, A.M. Comrie, *J. Chem. Soc.* 16 (1971) 2798.

[11] H.K. Mishra, *Arch. Pharm.* 316 (1983) 487.

[12] G. Sahin, E. Palaska, M. Ekizoglu, M. Ozalp, *IL Farmaco* 57 (2002) 539.

[13] H. Singh, L.D.S. Yadav, *Agric. Biol. Chem.* 40 (1976) 759.

[14] Y. Zheng, J. Lin, Y. Liang, Q. Lin, Y. Yu, Q. Meng, Y. Zhou, S. Wang, H. Wang, H. Zhang, *J. Mater. Chem.* 11 (2001) 2615.

[15] T. Sano, Y. Nishio, Y. Hamada, H. Takahashi, T. Usuki, K. Shibata, *J. Mater. Chem.* 10 (2000) 157.

[16] T. Noda, H. Ogawa, N. Noma, Y. Shirota, *J. Mater. Chem.* 9 (1999) 2177.

[17] X. Jiang, Y. Liu, H. Tian, W. Qiu, X. Song, D. Zhua, *J. Mater. Chem.* 7 (1997) 1395.

[18] Carella, A. Castaldo, R. Centore, A. Fort, A. Sirigu, A. Tuzi, *J. Chem. Soc., Perkin Trans.* 2 (2002) 1791.

[19] J. Wang, R. Wang, J. Yang, Z. Zheng, M.D. Carducci, T. Cayou, *J. Am. Chem. Soc.* 123 (2001) 6179.

[20] M.J. Frisch, G.W. Trucks, H.B. Schlegel, G.E. Scuseria, M.A. Robb, J.R. Cheeseman, G. Scalmani, V. Barone, B. Mennucci, G.A. Petersson, H. Nakatsuji, M. Caricato, X. Li, H.P. Hratchian, A.F. Izmaylov, J. Bloino, G. Zheng, J.L. Sonnenberg, M. Hada, M. Ehara, K. Toyota, R. Fukuda, J. Hasegawa, M. Ishida, T. Nakajima, Y.Honda, O. Kitao, H. Nakai, T. Vreven, J.A. Montgomery, Jr., J.E. Peralta, F. Ogliaro, M. Bearpark, J.J. Heyd, E. Brothers, K.N. Kudin, V.N. Staroverov, R. Kobayashi, J. Normand, K. Raghavachari, A. Rendell, J.C. Burant, S.S. Iyengar, J. Tomasi, M. Cossi, N. Rega, J. M. Millam, M. Klene, J.E. Knox, J.B. Cross, V. Bakken, C. Adamo, J. Jaramillo, R. Gomperts, R.E. Stratmann, O. Yazyev, A.J. Austin, R. Cammi, C. Pomelli, J.W. Ochterski, R.L. Martin, K. Morokuma, V.G. Zakrzewski, G.A. Voth, P. Salvador, J.J. Dannenberg, S. Dapprich, A.D. Daniels, O. Farkas, J.B. Foresman, J.V. Ortiz, J. Cioslowski, D.J. Fox, Gaussian 03, Revision C.02, Gaussian Inc., Wallinford, CT, 2004.

[21] Manju Pandey, S. Muthu, N.M. Nanje Gowda, *J. Mol. Struct.* 1130 (2017) 511.

[22] M.A. Morsy, A.M. Al-Somali, A.J. Suwaiyan, *Phys. Chem. B* 103 (1999) 11205.

[23] S.Y. Lee, B.H. Boo, *J. Phys. Chem.* 100 (1996) 15073.

[24] A.P. Scott, L. Radom, *J. Phys. Chem.* 100 (1996) 16502.

[25] M. Gussoni, C. Castiglioni, M.N. Ramos, M. Rui, G. Zerbi, *J. Mol. Struct.* 224 (1990) 445.

[26] R.M. Silverstein, F.X. Webster, D.J. Kiemle, Spectrometric Identification of Organic Compounds, seventh ed., Wiley, New York, 2005.

[27] B.H. Stuart, Infrared Spectroscopy: Fundamentals and Applications, John Wiley and Sons, Chichester, UK, 2004.

[28] M. Arockia doss, S. Savithiri, G. Rajarajan, V. Thanikachalam, C. Anbuselvan, *Spectrochim. Acta Part A,* 151 (2015) 773.

[29] S. Savithiri, M. Arockia doss, G. Rajarajan, V. Thanikachalam, *J. Mol. Struct.* 1075 (2014) 430.

[30] E. Scrocco, J. Tomasi, *Adv. Quantum Chem.* 11 (1979) 115.

[31] F.J. Luque, J.M. Lopez, M. Orozco, *Theor. Chem. Acc.* 103 (2000) 343.

[32] S. Savithiri, M. Arockia doss, G. Rajarajan, V. Thanikachalam, *J. Mol. Struct.* 1105 (2016) 225.

[33] H. Tanak, A.A. Agar, O. Büyükgüngor, *Spectrochim. Acta A,* 118 (2014) 672.

[34] M. Arockia doss, S. Savithiri, G. Rajarajan, V. Thanikachalam, H. Saleem, *Spectrochim. Acta Part A,* 148 (2015) 189.

[35] S. Savithiri , M. Arockia doss , G. Rajarajan , V. Thanikachalam , S. Bharanidharan , H. Saleem, *Spectrochim. Acta Part A* 136 (2015) 782.

[36] K. Gokula Krishnan, R. Sivakumar, V. Thanikachalam, H. Saleem, M. Arockia doss, *Spectrochimica Acta Part A,* 144 (2015) 29.

[37] K. Fukui, *Science* 218 (1982) 747.

[38] K. Fukui, T. Yonezawa, H. Shingu, *Chem. J. Phys.* 20 (1952) 722.

[39] C.H. Choi, M. Kertesz, *Chem. J. Phys.* 101A (1997) 3823.

[40] M. Kurt, P. Chinnababu, N. Sundaraganesan, M. Cinar, M. Karabacak, *Spectrochim. Acta A Mol. Biomol. Spectrosc.* 79 (2011) 1162.

[41] H. Nazır, M. Yıldız, H. Yılmaz, M.N. Tahir, D. Ulku, *J. Mol. Struct.* 524 (2000) 241.

[42] M. Nakano, I. Shigemoto, S. Yamada, K. Yamaguchi, *J. Chem. Phys.* 103 (1995) 4175.

[43] K. Wu, J.G. Snijders, C. Lin, *J. Phys. Chem. B* 106 (2002) 8954.